COMPARISON OF GROUND MOTIONS FROM CSN INSTRUMENTS AND PROXIMATE SENSORS FROM OTHER NETWORKS

Jonathan P. Stewart[1], Shako Mohammad[1], Chukwuebuka C. Nweke[2], Rashid Shams[2], Tristan E. Buckreis[1], Monica D. Kohler[3], and Yousef Bozorgnia[1]

[1] *UCLA Samueli Engineering*
[2] *USC Civil & Environmental Engineering*
[3] *California Institute of Technology*

Abstract

The Community Seismic Network (CSN) is a low-cost, MEMS-sensor seismic network with smaller average station-to-station spacing than stations for other networks. We have downloaded and processed CSN data for 29 earthquakes with **M** > 4 from 2012 to 2023 using NGA procedures. Visual checks of data useability were applied to distinguish rejected records form records with clear seismic signals. We compare recordings from proximate (within 3 km) CSN and non-CSN (generally SCSN or CSMIP) stations with usable signals. Results show no systematic differences for peak acceleration and similar spectra when the CSN motions have large usable bandwidths.

Introduction

The Community Seismic Network (CSN) is a network currently with over 800 three-component seismic stations, mainly in southern California (Clayton et al. 2011, 2020; http://csn.caltech.edu/), which are operated as a collaborative research effort between Caltech and UCLA. The network is expected to grow to 1200 three-component stations by the end of 2023. In terms of its layout and configuration, CSN differs from other seismic networks in two principal respects. First, the sensors are spatially concentrated in certain parts of southern California, and as a consequence, as currently configured they are relatively ineffective for some classical applications like earthquake location or recording motions over a wide distance range, but they are effective at capturing ground motion characteristics over relatively short length scales. Second, the instruments have relatively high noise levels compared to broadband seismometers or modern accelerometers.

We have recently completed a project that evaluated the effective noise threshold of CSN data based on the currently available recordings, to validate the recordings against those from higher-resolution sensors, and to make available in a public database CSN data that is judged to be reliable along with its associated metadata. Results of this study are presented in a project report (Stewart et al. 2023). This paper presents a portion of the research results related to comparisons of CSN data to data from proximate sensors from alternate networks (mainly CSMIP and Southern California Seismic Network).

Following this introduction, we provide background information on the CSN, describe the data produced by the network, describe the data processing and assignment of classes that indicate record quality, and compare CSN data to data from other networks.

CSN Instruments and Housing

Over the duration of the current project, the Community Seismic Network (CSN) comprised 769 seismic station locations, most of which are in southern California (Clayton et al., 2020). In addition, there are 339 previously active but now decommissioned station locations, some of which produced data that is evaluated. Figure 1 shows the locations of CSN stations overlaid on a regional map that also shows stations from other regional networks (CSMIP, USGS, SCSN). As indicated in Figure 1, the locations of CSN stations include the San Fernando Valley, Pasadena, San Gabriel Valley, downtown Los Angeles, Hollywood, and South Los Angeles; many of these areas have high densities of population or industrial activity and hence are culturally noisy.

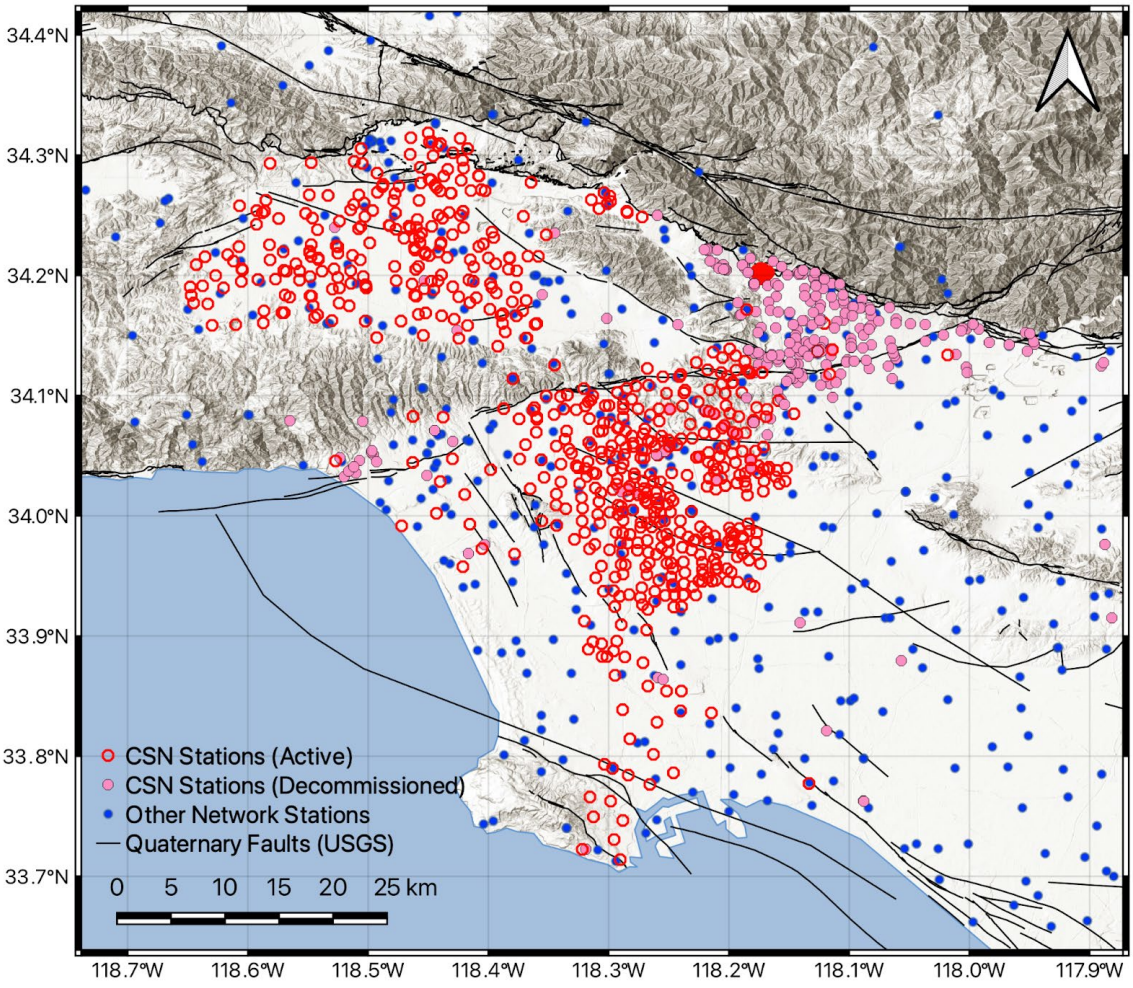

Figure 1. Map of southern California showing locations of ground motion stations considered in prior work (NGA-West2, Bozorgnia et al. 2014 & basin study, Nweke et al. 2022) (CSMIP, USGS, SCSN) and CSN stations (active and decommissioned) considered in this project.

CSN utilizes low-cost, three-component, MEMS accelerometers. The primary product of the network is measurements of shaking of the ground as well as upper floors in buildings, in the seconds during and following a major earthquake. Each sensor uses a small, dedicated ARM processor computer running Linux, and analyzes time series data in real time at 250 samples per second (sps), which is then downsampled to 50 sps. Innovations in cloud computing for data processing, coupled with sensor developments for the video-gaming and automotive air bag industries, have helped form the technological basis of this network. Prior to ~2014, most CSN stations consisted of plug-in sensors that were attached to community hosts' laptops and desktop computers; the hosts determined the deployment location and coupling. Data from these deployments went into the early earthquake database, but this deployment type no longer exists. After 2014, all CSN sensors are stand-alone devices deployed by a CSN field engineer who determines location and physical coupling with the floor.

Some CSN station locations have multiple instruments. This occurs because of multiple instruments (referred to here as a "station") within a structure at different heights, and in some cases, different locations in plan at a given height. The number of three-component instruments is 1868, which includes 1250 ground stations, 27 basement stations, and 463 stations on floors of buildings above the ground line. The instrumented buildings have between 1 and 3 triaxial sensors deployed per floor. The sensing hardware and parameters are the same as for the free-field. There are no sensors on lifelines infrastructure at the present time.

We focused on ground and basement stations and do not consider above-ground stations. Each of the ground-level and basement stations has been assigned an instrument housing code using guidelines from COSMOS (COSMOS 2001). This information is provided as metadata accompanying the CSN sites in the ground motion database (Buckreis et al. 2023). The applicable codes that were applied to CSN stations are as follows:

1. "04" - ground-floor in a 1-2 story building without a basement (1250 CSN stations)
2. "05" - ground-floor in a larger structure (118 CSN stations)
3. "09" - basement or underground in a large vault (27 CSN stations)
4. "10" - upper levels of a structure (463 CSN stations)

Stations in group 04 can be considered "free-field." Stations in 05 and 09 might be approximated as free-field depending on the depth of embedment (for 09) and plan size of the structure (for 05). The difference between the 769 figure mentioned at the start of this section and the sum of 04, 05, and 09 is caused by the occurrence of multiple stations at a given site at the ground level or basement level.

Database

Events Considered

Figure 2 shows the locations of 29 events considered in this study. We include all events recorded by the network with **M** > 4. Per NGA protocols (e.g., Contreras et al. 2022), seismic

moment is taken from the global centroid moment tensor catalog (Ekström et al. 2012; https://www.globalcmt.org/) as are other moment tensor attributes with the exception of hypocenter location, which is taken from USGS (https://www.usgs.gov/programs/earthquake-hazards/earthquakes).

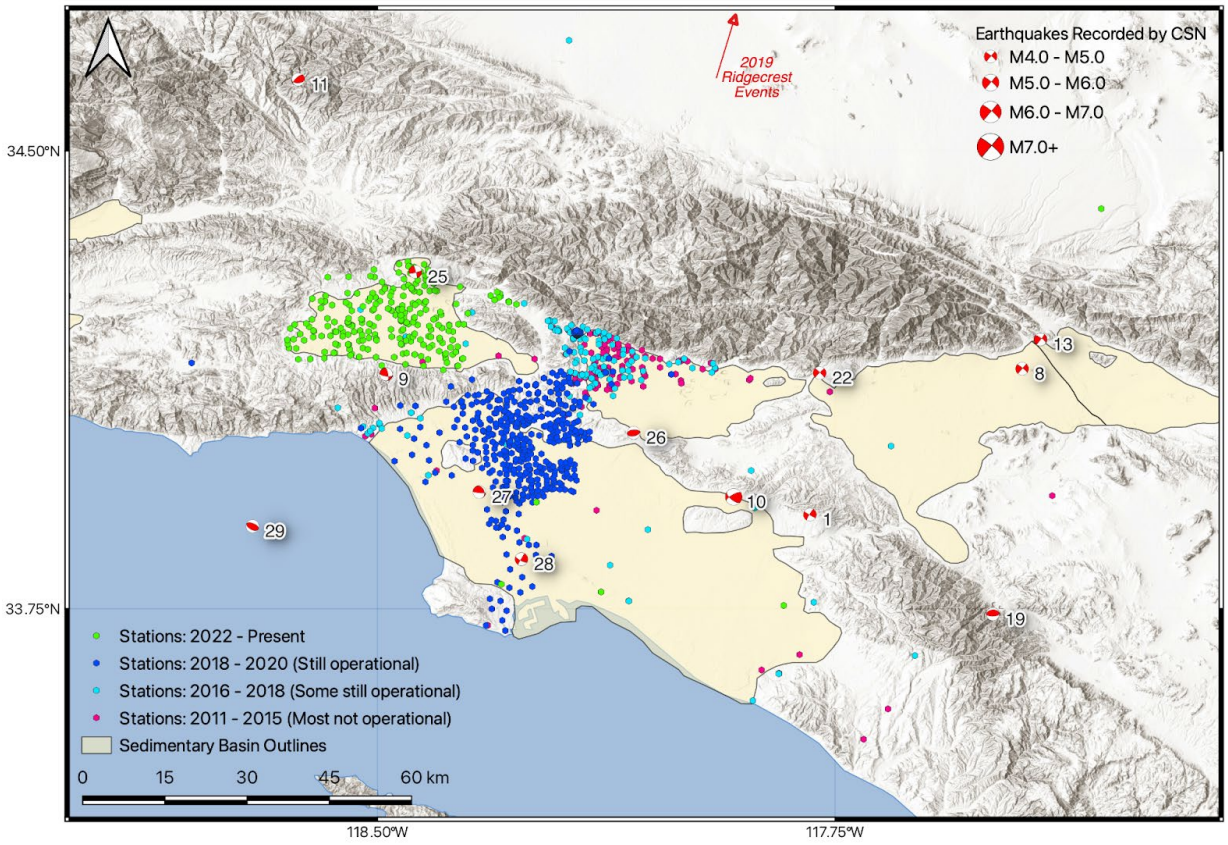

Figure 2. Map of CSN stations and the events they recorded.

CSN Data Processing

The Next Generation Attenuation (NGA; e.g., Bozorgnia et al 2014) program has developed standard steps that are used to process earthquake ground motions. The aim of the steps is to minimize the effects of noise on recorded ground motions, while optimizing the dynamic range for which a given recording can be considered to accurately represent the ground shaking at the site. The most recent procedures are described by Goulet et al. (2021) and Kishida et al. (2020), although the main elements of the procedure were presented earlier by Boore (2005), Boore and Bommer (2005), and Douglas and Boore (2011). The steps included the following, and are illustrated by Stewart et al. (2023) for their application to the CSN data:

1. Screening to identify noise-dominated records or records with spurious features
2. Identification of noise and signal windows

3. Compute Fourier Amplitude Spectra (FAS) of both windows and normalization of the FAS to account for potentially different window durations.
4. Apply high- and low-pass filters to minimize effects of noise at low and high frequencies, respectively.
5. Baseline correction

These procedures were applied using a modified version of the gmprocess code (Hearne et al., 2019). As described in Ramos-Sepulveda et al. (2023), the modifications improve the high-pass corner frequency selection to minimize displacement wobble and facilitate human review and modification of corner frequencies.

Some of the events shown in Figure 2 were not present in the working version of the relational ground motion database being used in the NGA-West3 project (Buckreis et al. 2023). For those events, non-CSN data was also processed using similar procedures so that more complete datasets for each event are available. All of the data is incorporated into the current working version of the database, which is publicly available.

Data Classification

In our evaluations of the CSN data, we observed three general categories of records. The "best" records (BroadBand Records; BBR) clearly reflect earthquake shaking, having waveforms where the different wave arrivals are evident and modest effects of noise. Records deemed unusable (REJected records; REJ) appear to be noise dominated, generally based on visual inspection of time series, but sometimes also from similar levels of signal and noise FAS. The intermediate case (Narrow-Band Records; NBR) consists of records that have the visual appearance of earthquakes, but the signal is of modest strength in comparison to noise and the record bandwidths are relatively limited.

Figure 3 shows data distributions in magnitude-distance space for BBR (green), NBR (yellow), and REJ (red) records. In the upper-left portion of the plot (large magnitude or close distances for **M** < 5 events), most records are BBR, whereas the lower-right portions (**M** < 5 event and distances > 50-100 km) are REJ. Clearly the level of ground shaking strongly affects the classifications. This is also reflected in summary statistics for the data set. Among events since 2018, large-magnitude events and events generally closer than 70-80 km from the network (Malibu, Carson, Lennox, El Monte, Pacoima, Searles Valley, Ridgecrest, La Verne) have the following aggregate component record classifications:

- Usable records (BBR and NBR): 5470 (56.7%) (1122 BBR, 4358 NBR)
- Rejected records: 4176 (43.2%)

The database as a whole, which includes many events with small magnitude and large distances, breaks down as

- Usable records (BBR and NBR): 9286 (46.4%) (1187 BBR, 8009 NBR)
- Rejected records: 10,612 (53.6%)

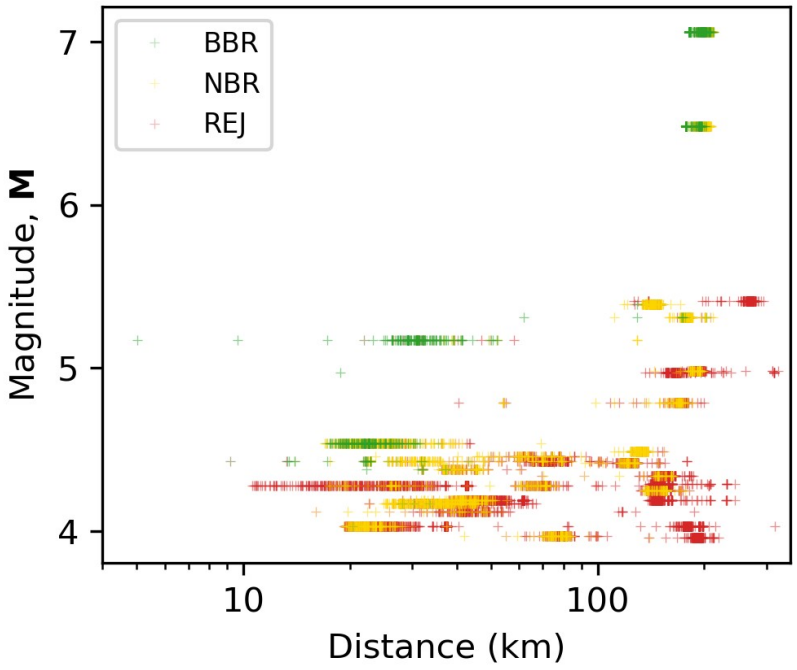

Figure 3. Record classification as function of distance and magnitude.

Data Comparisons

An important step in the evaluation of the usability of ground motions recorded by CSN stations is to compare with ground motions recorded by non-CSN/traditional network sensors that have been used in previous studies (i.e., NGA projects). Such comparisons are most robust when sensors from both networks share the same location and both record a given event. Three such co-located sensor pairs exist in the network. The analysis of these sensors (Stewart et al. 2023) is inconclusive due to the small size of the data set and some differences in the sizes of structures housing the different instruments. Here, we instead focus on proximate sensors, which meet two criteria: (1) the stations are separated by ≤ 3 km and (2) the stations have the same surface geology, based on the statewide map by Wills et al. (2015). Station pairs that meet these criteria are mapped in Figure 4 (arrows are drawn between paired stations).

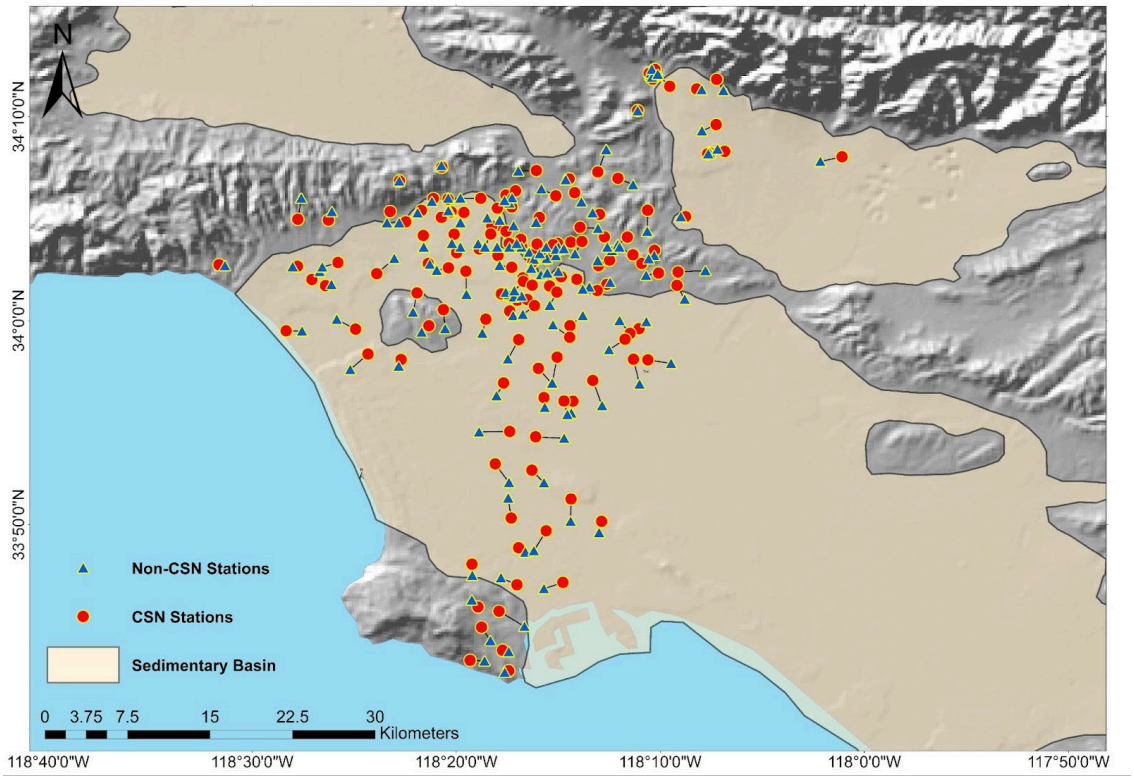

Figure 4. Map showing proximate CSN and non-CSN stations (160 pairs), defined by separation distances ≤ 3 km and matching surface geologies as provided by Wills et al. (2015).

For each station pair, a differential ground motion IM is computed as:

$$\delta(lnIM) = ln(IM_{csn}) - ln(IM_{net}) \quad (1)$$

where the 'csn' subscript indicates the IM is from the CSN station and the 'net' subscript indicates the IM is from the non-CSN station. Both IMs are taken from individual as-recorded components of ground motion (generally north-south and east-west). The average value of $\delta(lnIM)$ is denoted μ_δ.

Figure 5 plots $\delta(lnIM)$ vs separation distance for cases in which the CSN records are BBR and the IM is PGA. The mean difference in this case is μ_δ = -0.017 with a standard error of the mean of 0.071. These results show that the CSN PGAs are on average slightly smaller than the non-CSN PGAs, but that the differences are small and within the margin of error. Figure 6 shows the variation of $\delta(lnIM)$ with period for Sa over the period range of 0.01 to 10 sec. Data are only considered in the calculation of the binned means when both the CSN and non-CSN Sa values are within their usable ranges given the data filtering (i.e., the oscillator period T < 0.8/f_{cHP} for both instruments). The results in Figure 6 show a negative bias (CSN lower) for periods near 1.0 sec (~0.6 < T < 2.0 sec) and for T > ~5 sec, but otherwise the two sets of IMs essentially match. The bias near 1.0 sec is about 10-15% (-0.1 to -0.15 ln units).

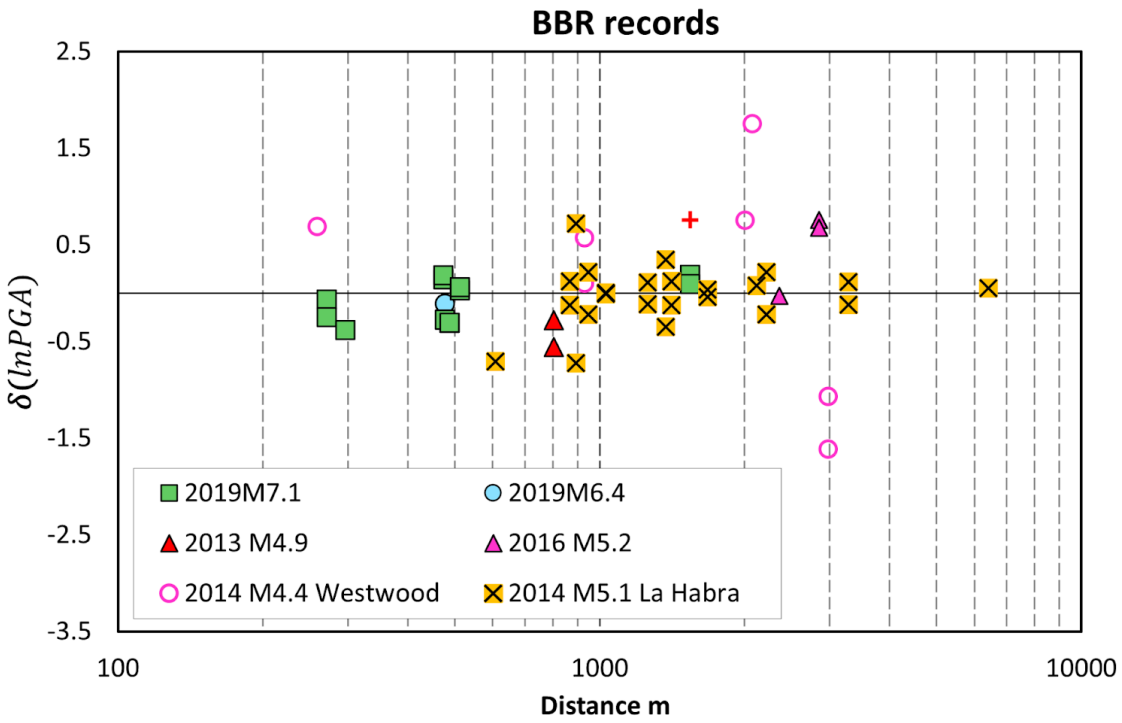

Figure 5. Variation of differential PGA with station separation distance for BBR CSN recordings. The mean and standard deviation of the data are μ_δ = -0.017± 0.071

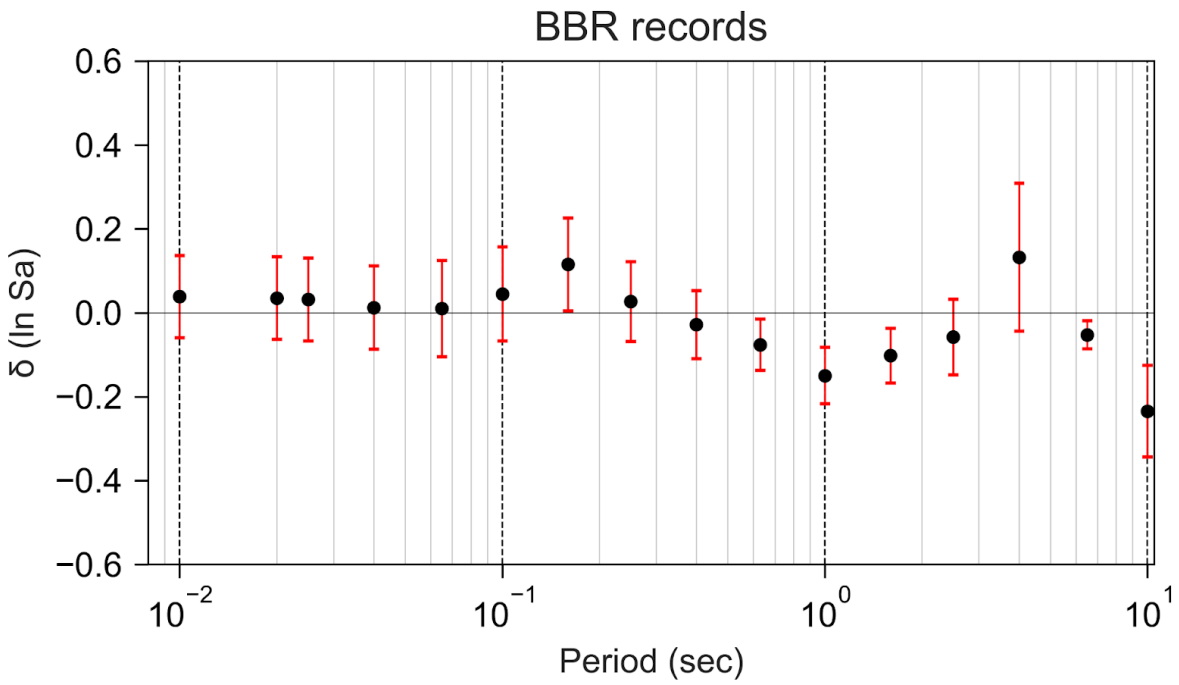

Figure 6. Variation of mean differential Sa with period for BBR CSN recordings

Figure 7 plots $\delta(lnIM)$ vs separation distance for cases in which the CSN records are NBR and the IM is PGA. The mean difference in this case is μ_δ = -0.023 with a standard error of the mean of 0.056. These results show that the CSN PGAs are on average smaller than the non-CSN PGAs, but as with BBR data, the differences are small enough that the bias can be considered to be statistically insignificant. Figure 8 shows the variation of $\delta(lnIM)$ with period for Sa over the period range of 0.01 to 10 sec. The results in Figure 8 show a negative bias (CSN lower) over multiple period intervals including 0.05-0.1 sec, 0.4-1.0 sec, and > 3 sec. Within these period intervals, the levels of bias are small (~ -0.1 ln units) but are repeatable and statistically significant.

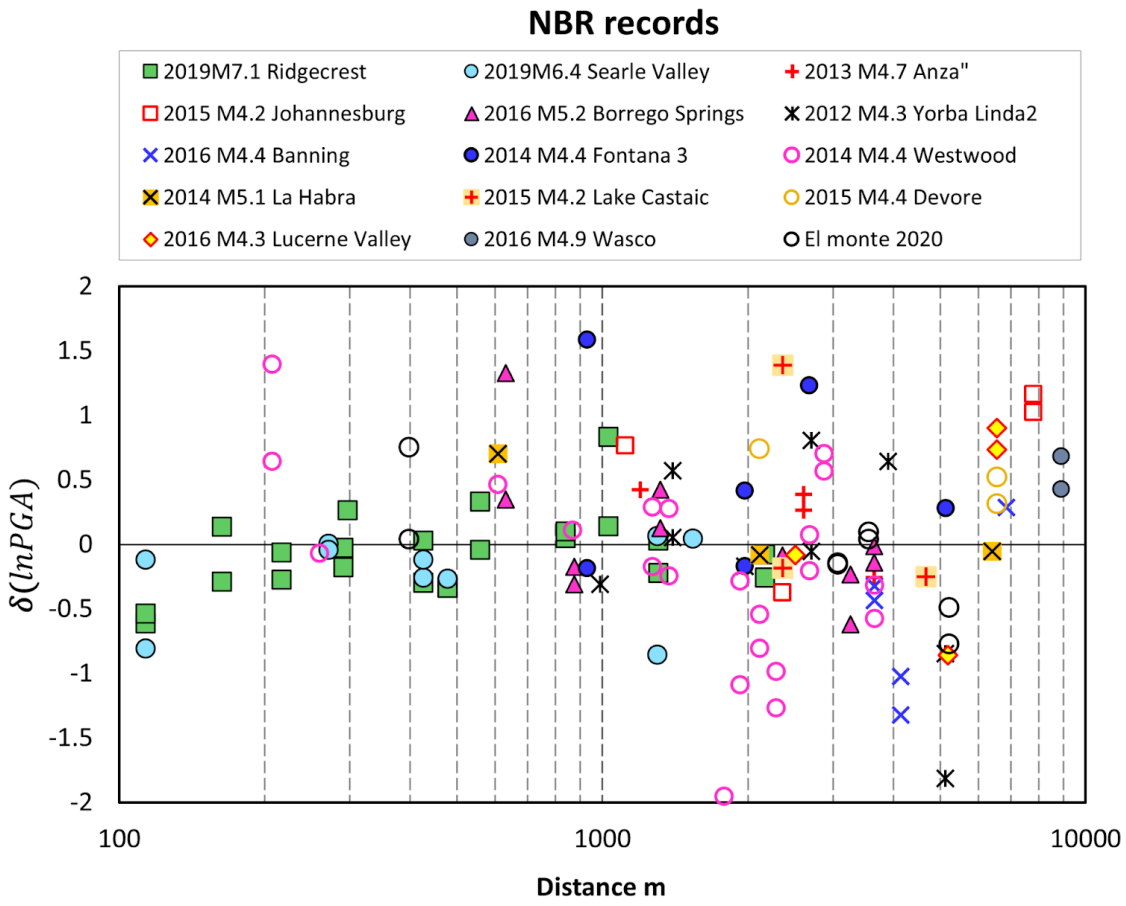

Figure 7. Variation of differential PGA with station separation distance for NBR CSN recordings. The mean and standard deviation of the data are μ_δ = -0.023± 0.056

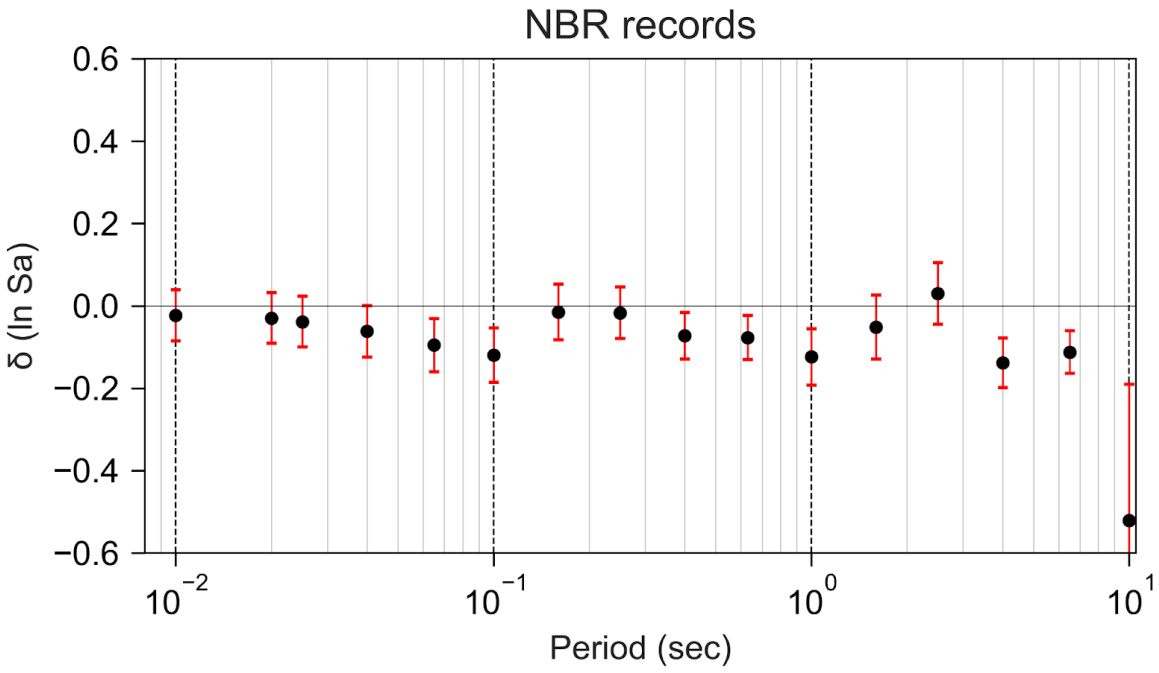

Figure 8. Variation of mean differential Sa with period for NBR CSN recordings.

The results presented above show that BBR CSN and non-CSN records are similar within the typical usable period range of PGA to ~5 sec, with the exception of low CSN ground motions near 1.0 sec. The CSN NBR records are also unbiased for PGA, but these records have lower ground motions than the non-CSN records over a range of periods, which is expected because by definition these records have a relatively limited frequency range and hence are missing significant portions of the seismic signal at low and high frequencies. As a result, we suggest that the criteria used to define BBR recordings be used to identify usable CSN data for ground motion applications.

Conclusions

This broader study from which the Stewart et al. (2023) report was produced has undertaken a series of tasks that collectively aim to provide insight into the performance of CSN ground-level sensors during southern California earthquakes, provide processed data in an accessible form for users, and provide recommendations on the range of conditions for which the data can be used with confidence in ground motion modeling projects.

CSN data from 29 earthquakes was uniformly processed using NGA-type procedures. For events where data from other networks was already available, the CSN data has been added to a national database for ground motion research applications (Buckreis et al. 2023) to supplement the previously available data. For events not previously in the database, CSN and non-CSN data has

been processed and added to the database. Relevant site and event metadata has been compiled and added so that this data is available for public use.

Among the events considered, approximately 50% of the recordings were judged to be not usable because they are noise-dominated based on visual inspection or have unusual features. These are referred to as REJ records in this report. However, this rate is potentially misleading as an indicator of network performance, because 27 of the 29 events are small magnitude (< 5.5) and often occurred at considerable distances from the network. Two large events (2019 Searles Valley and 2019 Ridgecrest) were successfully recorded by over 95% of sensor horizontal components, despite being located at distances > 150 km. This rate of data recovery is considered more representative of the performance that can be expected in future impactful earthquakes in the greater Los Angeles area.

Among the remaining (non-REJ) recordings, we distinguished records with relatively broad bandwidth (usable Fourier frequency range of at least 0.5 - 10 Hz) (denoted BBR) from those with relatively limited bandwidth (narrower than that for BBR at one or both ends of the frequency range; denoted NBR). Comparisons of BBR and NBR signals with signals from non-CSN proximate sensors (separation distance < 3 km and same geology) shows that PGA levels are not statistically distinguishable. Spectral accelerations from BBR CSN data appear to be unbiased over the oscillator period range of 0.01 to 5 sec based on these comparisons with the exception of lower CSN motions near 1.0 sec, whereas NBR CSN data have lower spectral accelerations for multiple period intervals < 5 sec (amount of the bias is generally < 10-15%). This is not surprising given the limited bandwidth of NBR signals.

These results show that CSN data is useful for research and engineering applications, but its range of applicability is more limited than data from more sensitive instruments. Within its application range, the CSN data have advantageous features, including relatively small between-sensor spacings that facilitate site response or ground motion variability studies at short length scales, as well as its continuous recording of ground motions. We strongly encourage continued operation and explanation of the CSN network to facilitate these and other research applications.

Acknowledgments

Funding for this study was provided by the California Strong Motion Instrumentation Program under contract number 1021-006. Partial support for the second and fourth authors was also provided by the UCLA and USC Civil & Environmental Engineering Departments, respectively. This support is gratefully acknowledged. The work presented here represents the views and opinions of the authors and does not reflect the policy, expressed or implied, of the State of California or the University of California. Helpful input was received during the project from Eric Thompson, Scott Brandenberg, and Maria Ramos-Sepulveda.

References

Boore DM, 2005. On pads and filters: processing strong-motion data, *Bull. Seism. Soc. Am.*, 95, 745-750.

Boore DM and Bommer JJ, 2005. Processing of strong-motion accelerograms: Needs, options and consequences, *Soil Dynamics & Earthquake Engineering*, 25, 93-115

Bozorgnia Y, Abrahamson NA, Al Atik L, Ancheta TD, Atkinson GM, Baker JW, Baltay A, Boore DM, Campbell KW, Chiou BS-J, Darragh RB, Day S, Donahue JL, Graves RW, Gregor N, Hanks T, Idriss IM, Kamai R, Kishida T, Kottke AR, Mahin SA, Rezaeian S, Rowshandel B, Seyhan E, Shahi S, Shantz T, Silva WJ, Spudich P, Stewart JP, Watson-Lamprey J, Wooddell KE and Youngs RR. 2014. NGA-West2 Research Project. *Earthquake Spectra* 30: 973–987.

Buckreis, TE, Nweke CC, Wang P, Brandenberg SJ, Mazzoni S, Stewart JP, 2023. Relational database for California strong ground motions, Geo-Congress 2023: Geotechnical Data Analysis and Computation, Los Angeles, CA, March 2023, *Geotechnical Special Publication No. 342*, EM Rathje, B Montoya, and MH Wayne (Eds.), 461-470, ASCE Geo-Institute

Clayton R, Heaton T, Chandy M, Krause A, Kohler M, Bunn J, Guy R, Olson M, Faulkner M, Cheng MH, Strand L, Chandy R, Obenshain D, Liu A, and Aivazis M, 2011. Community Seismic Network, *Annals of Geophysics*, 54 (6), doi: 10.4401/ag-5269.

Clayton R, Kohler M, Guy R, Bunn J, Heaton T, and Chandy M, 2020. CSN/LAUSD network: A dense accelerometer network in Los Angeles schools, *Seis. Res. Lett.*, 91(2A), 622-630, doi:10.1785/0220190200.

Contreras V, Stewart JP, Kishida T, Darragh RB, Chiou BSJ, Mazzoni S, Youngs RR, Kuehn NM, Ahdi SK, Wooddell K, Boroschek R, Rojas F, Ordenes J, 2022. NGA-Sub source and path database, *Earthquake Spectra*, 38(2), 799-840.

Consortium of Organizations for Strong-Motion Observation Systems (COSMOS), 2001 COSMOS strong motion data format. https://www.strongmotioncenter.org/vdc/cosmos_format_1_20.pdf (last accessed 9/15/2023).

Douglas J and Boore DM, 2011. High-frequency filtering of strong-motion records, *Bull. Eqk. Eng.*, 9, 395–409.

Ekström G, Nettles M, Dziewonski AM, 2012. The global CMT project 2004–2010: Centroid-moment tensors for 13,017 earthquakes. *Physics the Earth and Planetary Interiors* 200–201: 1–9.

Goulet, CA, Kishida T, Ancheta TD, Cramer CH, Darragh RB, Silva WJ, Hashash YMA, Harmon J, Parker GA, Stewart JP, Youngs RR, 2021. PEER NGA-East database, *Earthquake Spectra*, 37(S1), 1331-1353

Hearne M, Thompson EM, Schovanec H, Rekoske J, Aagaard BT and Worden CB, 2019. USGS automated ground-motion processing software, USGS Software Release, doi:10.5066/P9ANQXN3.

Kishida T, Darragh RB, Chiou BSJ, Bozorgnia Y, Mazzoni S, Contreras V, Boroschek R, Rojas F, Stewart JP, 2020. *Chapter 3: Ground motions and intensity measures (Data resources for NGA-subduction project)* (ed JP Stewart). PEER report 2020/02. Berkeley, CA: Pacific Earthquake Engineering Research Center, UC Berkeley.

Nweke CC, Stewart JP, Wang P, Brandenberg SJ, 2022. Site response of sedimentary basins and other geomorphic provinces in southern California, *Earthquake Spectra*, 38(4), 2341-2370.

Ramos-Sepulveda ME, Parker GA, Thompson EM, Brandenberg SJ, Li M, Ilhan O, Hashash YMA, Rathje EM and Stewart JP, 2023. High-pass corner frequency selection for implementation in the USGS

automated ground-motion processing tool, Geo-Congress 2023: Geotechnical Data Analysis and Computation, Los Angeles, CA, March 2023, Geotechnical Special Publication No. 342, EM Rathje, B Montoya, and MH Wayne (Eds.), 327-335, ASCE Geo-Institute

Stewart, JP, Mohammad S, Nweke CC, Shams R, Buckreis TE, Kohler MD, Bozorgnia Y (2023). Usability of ground motions recorded by Community Seismic Network, Garrick Institute for Risk Sciences, UCLA Samueli Engineering.

Wills CJ, Gutierrez CI, Perez FG, Branum DM, 2015. A next generation VS30 map for California based on geology and topography, *Bulletin of the Seismological Society of America* 105(6): 3083–3091.